JOURNAL OF MATERIALS SCIENCE 33 (1998) 3999–4005

Mechanical properties of nanocomposite organosilicate films

P. ETIENNE, J. PHALIPPOU, R. SEMPERE
Laboratoire des Verres, U.M.R. CNRS N°5587, Université de Montpellier II, 34095 Montpellier Cedex 5, France
E-mail: petienne@crit.univ-montpe.fr

Nanocomposite coatings have been deposited on plastic substrates by the dipping–drawing technique. The coatings were constituted by a matrice of a hybrid organomineral gel and a reinforcement made of amorphous silica. Two methods by which increase the silica content were investigated: silica was added via a silicon alkoxide compound or via dense silica particles of 10 nm size. Young's modulus and the hardness of the coating were measured using home-built equipment, and results compared to literature models. It is shown that the agreement between models and experimental values depends on the method of preparation of the nanocomposite coating. On the other hand, deviations appear when the volume fraction of reinforcement surpasses the three-dimensional percolation threshold.

1. Introduction

Transparent plastics are good candidates for optical applications. They have a low density and their impact resistance is much higher than that of inorganic glasses. However, they are not scratch resistant and, consequently, they rapidly loose their optical properties [1].

A thin layer of inorganic compound can be deposited on a substrate by the sol–gel process [2]. Coating is performed by dipping and then drawing a substrate out of a liquid which gels at room temperature [3]. Both aqueous and organic solutions are used. The gel results from a polycondensation reaction which usually occurs between hydroxyl groups [4]. After drying at room temperature, the gel forming the coating is porous and its mechanical properties are quite poor; baking is necessary to densify the coating. This thermal treatment is easily carried out when the substrates are temperature-resistant materials. However, such a thermal treatment is not possible when the substrate is an organic polymer which cannot tolerate temperatures higher than 150 °C. Moreover, experiments show that an inorganic layer prepared from the sol–gel process does not adhere to the substrate without previous chemical treatment.

Adherent and dense films may be obtained using chemical precursors which associate both organic and inorganic functions [5]. These hybrid materials present mechanical properties close to that of organic polymer compounds. They behave as polymers, showing an elastic response to very low stresses while they become plastic for high applied loads.

To improve the scratch resistance, tribology experiments have been previously undertaken [6]. It was shown that the scratch resistance is a complex mechanism which depends on the nature of the debris which is interposed between the material and the steel pin.

Recent investigations have shown that the erosion rate (thickness removed by unit time) mainly depends on three mechanical properties: Young's modulus, E, hardness, H, and the critical stress intensity factor, K_{IC} [7]. It is foreseen that in the future, coatings will be composites constituted by at least two components; however, coating properties must be previously established as a function of coating composition.

The present work investigated the variation of elastic modulus and hardness as a function of the coating composition. Young's modulus is usually measured on a macroscopic scale by subjecting the material to an applied stress. Two methods are used. The first one is a dynamic method, consisting of fitting the frequency excitation to the coated substrate frequency resonance [8]. When a sample is non-magnetic or non-conductive, some authors placed the sample directly on a vibrating membrane (loud speaker) [9]. Another dynamic method consists of measuring the speed of ultrasonic waves which propagate in the coating (Rayleigh waves) [10]. These techniques require a precise measurement of the frequency of the sound velocity. Furthermore, a precise value of the thickness and density of the layer is often required to calculate Young's modulus of the coating. An accurate measurement of the coating density is not often easily performed.

Static methods are the second way to evaluate Young's modulus. They consist of loading the specimen and measuring the strain. According to the specimen geometry, Young's modulus of the coating may be estimated if Young's modulus of the substrate is known. In the case of a brittle material, this experiment is advantageously performed by a bending technique [11].

However, this technique requires knowledge of the elastic constant of the substrate. A more recent method has been proposed to evaluate the elastic property of coating [12, 13], based on a precise measurement of the penetration depth on an indentor into the layer. The indentor must have a well-defined geometry [14]. It was shown that the mechanical response is due to the pure layer as long as the investigated penetration does not exceed 10% of the whole layer thickness.

This method permits evaluation of both the elastic property (Young's modulus) and the plastic behaviour which is directly related to the layer hardness [15]. With respect to the small investigated area, this technique allows the coating homogeneity to be assessed by performing several runs at different locations on the coating surface.

2. Experimental procedure

2.1. Sample preparation

The substrate, poly(diethylene glycol dialyl *bis* carbonate), is a transparent plastic obtained by radical polymerization induced by a thermal treatment performed at 90 °C. The substrate was 1 mm thick, with a Young modulus of 2.3 ± 0.1 GPa and a microhardness of 246 MPa.

The coatings were prepared by dipping the substrates in a solution and drawing them at a speed of 10 cm min^{-1}. Dipping was carried out at room temperature under a moisture controlled atmosphere (50% RH).

The solutions contained a γ-glycidoxypropyltrimethoxysilane (GPTMS) as a base compound to which other elements were added. GPTMS, which belongs to the ORMOSIL® family, plays different roles. It may be considered as a coupling agent to the plastic substrate, allowing good adhesion of the coating. It may also play the role of a forming system for both organic and inorganic networks. While the inorganic part (Si-OMe) of the molecule may establish a silica network through hydrolysis and polycondensation reactions, the organic network results of the epoxy bonds cleavage. To this compound, a quantity of chemical species, which theoretically can be transformed into an inorganic compound (SiO_2), is added. Silica may be formed from tetramethoxysilane, TEOS (A), or directly added as colloidal particles, 10 nm in size. These colloidal particles are stabilized and diluted in a methanolic solution (B). The coating composition depends on the nature of the mineral part (series A for TEOS and series B for colloidal silica). For series A, the TEOS is assumed to be totally transformed into silica. Finally, the coating properties may be varied according to the relative amounts of silica and GPTMS. Compositions are given in silica per cent, assuming that the source of silica from silicon atoms borne by GPTMS can be neglected. Details of solution preparation are given in Fig. 1.

The film layer was dried at 60 °C for 15 min. Polymerization was then performed at 100 °C for 3 h. For silica contents higher than 40% (series A) and 50% (series B), coatings were no longer homogeneous.

The sample geometry was beams of $50 \times 5 \times 1\,mm^3$. Beams were prepared from 70 mm diameter dishes,

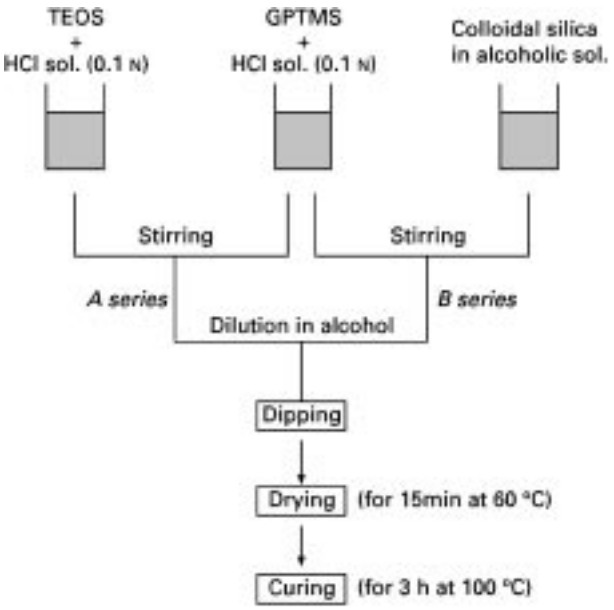

Figure 1 Sample preparation.

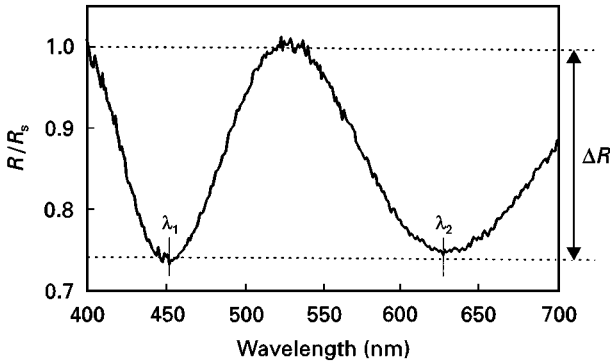

Figure 2 Experimental visible reflection spectroscopic curve. *R* represents the coating reflection.

with the length (50 mm) was taken perpendicular to the drawing direction. The extremities were discarded to avoid coating thickness variation which appears at the edge of the dishes.

2.2. Sample characterization

The coating thickness was measured using reflection spectroscopy in the visible range. The measurement requires recording of both the reflection spectra of the bare substrate, R_S, and of the covered substrate, R_C. The calculated ratio, R_C/R_S, allows the spectrum of the source to be eliminated. The obtained curve (Fig. 2) shows perfectly defined and located extrema which allow the coating thickness, h_C, to be estimated from the relationship

$$h_C = \frac{j\lambda_1\lambda_2}{2n_C(\lambda_1 - \lambda_2)} \quad (1)$$

where j is the total number of minima counted within the spectral range between λ_1 and λ_2. n_C is the refractive index of the coating

$$n_C = \left[n_0 n_S \frac{1 + (|\Delta R| \times R_S)^{1/2}}{1 - (|\Delta R| \times R_s)^{1/2}} \right]^{1/2} \quad (2)$$

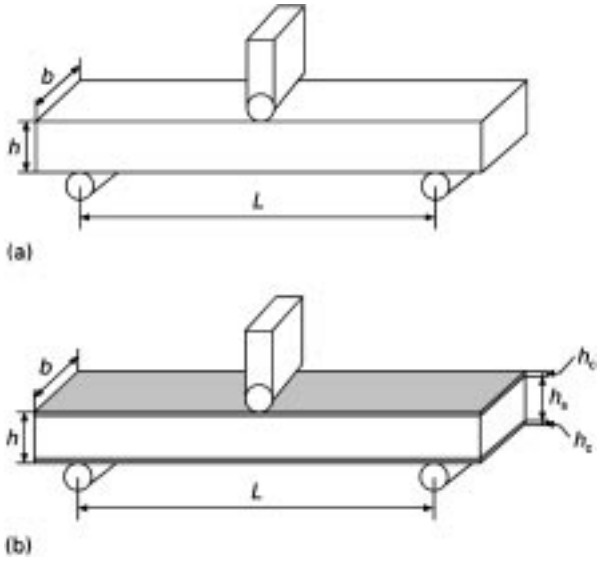

Figure 3 Three-point bending experiments on (a) a bare (BS) and (b) a covered (CS) substrate.

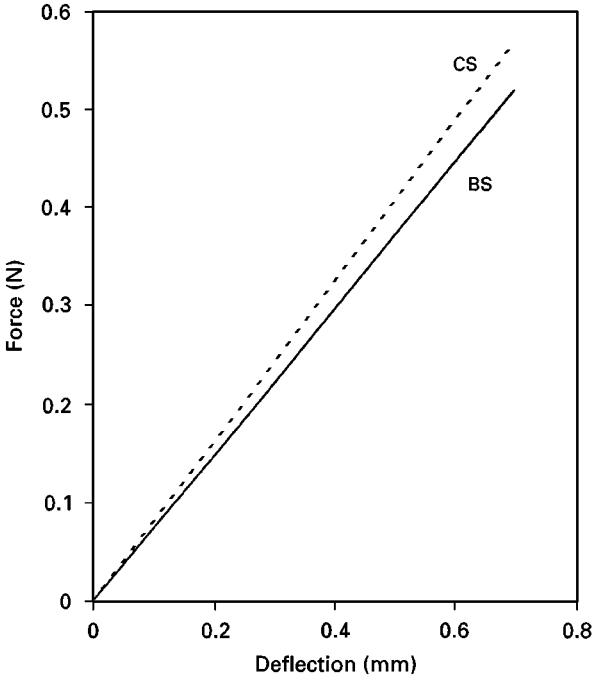

Figure 4 Comparison of deflection–force curves on a bare (BS) and covered (CS) substrate.

where ΔR is the difference between a maximum and a minimum. R_S is given by

$$R_S = \left(\frac{n_S - n_0}{n_S + n_0}\right)^2 \tag{3}$$

where n_S and n_0 are the refractive index of bare substrate and atomosphere, respectively.

The coating thickness varies between 2 and 5 μm and the refractive index between 1.49 and 1.5, depending upon the composition and nature of the coating.

The elastic modulus of the coating was estimated using two methods. The first one is the three-point bending method [16]. Fig. 3 shows the geometrical parameters of the sandwich which deforms, d, under the action of the applied load, F. Assuming a perfect adhesion between the substrate and coating, the sandwich Young's modulus, E, is related both to that of the coating, E_C, and of the bare substrate, E_S, using the relationship (see the Appendix).

$$E = E_S \frac{h_S^3}{(h_S + 2h_C)^3} + 2E_C \frac{h_C^3}{(h_S + 2h_C^3)} + 6E_C \frac{h_C(h_S + h_C)^2}{(h_S + 2h_C)^3} \tag{4}$$

where the subscripts S and C refer to the substrate and coating, respectively. Such a calculation requires precise measurement of the load and the associated deflection. These data are recorded using a precision home-built apparatus. A detailed account of the apparatus used has been given elsewhere [11]. A typical curve is shown in Fig. 4.

The other method to evaluate Young's modulus of the coating is provided by an indentation measurement. The experimental inverse indentor (Fig. 5) was built with analogous sensors to those used for the three-point machine. However, to measure precisely the penetration depth, the target (which is usually made of steel) was made of copper. This material induces greater changes in the electromagnetic field

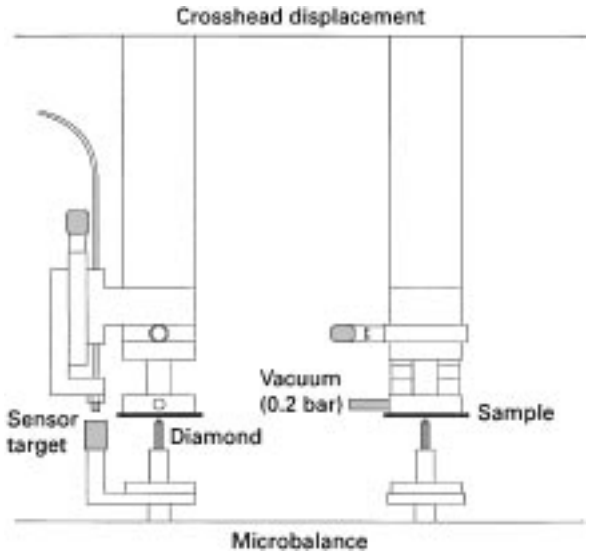

Figure 5 Experimental apparatus for the indentation.

for the inductive sensor. The measurement scale was about 100 μm, with an accuracy of 1 nm. The indentor was a pyramid-shaped diamond with a triangular base. With such a geometry the hardness, H, is related to the depth penetration, e, by the relationship

$$H = 0.0377 \frac{F}{e^2} \tag{5}$$

where F is the applied load. A typical curve obtained on the bare substrate is given in Fig. 6. The mechanical response then corresponds to elastic release while plasticity is not accounted for. At the onset of unloading, the curve is linear, because the contact area between the sample and the indentor remains constant. The value of the slope corresponds to the stiffness, S, of the two bodies in contact. The stiffness is

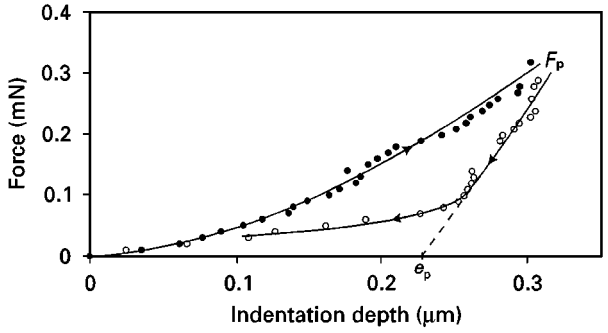

Figure 6 Indentation curve on a bare substrate.

related to Young's modulus [12] of the sample and of the indentor by the relations

$$S = \frac{dF}{de} = 2E\left(\frac{A}{\pi}\right)^{1/2} \quad (6)$$

where e is the depth, and

$$\frac{1}{E} = \frac{1 - \nu_S^2}{E_S} + \frac{1 - \nu_D^2}{E_D} \quad (7)$$

where A is the contact area between indentor and the sample. The subscript S and D refer, respectively, to the sample and the diamond, ν is Poisson's coefficient. Extrapolation of the slope to a theoretical zero value of the load gives the plastic indentation depth, e_p. This value corresponds to the depth of the diamond fingerprint which should be obtained if the sample was purely plastic. According to this indentation depth, plastic hardness, can be defined.

When the experiment is carried out on a coated surface and if the penetration depth does not exceed 10% of the coating thickness, the coating modulus can be obtained.

The reported value is the average calculated from five experiments. The error bar corresponds to that estimated from STUDENT [17] method with a confidence interval of 95%.

3. Experimental Results

Young's modulus values of the coating obtained from indentation experiments are a little lower than those obtained from the three-point bending experiments (Fig. 7). However, with respect to the error bar, the results are considered to be identical. For further calculations, a mean value between these two methods will be used.

As expected, the elastic modulus increases with silica content. It is noteworthy that coatings prepared with colloidal silica (B) show a lower elastic modulus than those prepared with TEOS (A). A comparison can be made between these two kinds of coating, assuming that TEOS is totally transformed into silica. For silica contents higher than 25%, the difference becomes more and more pronounced.

Hardness measurements which are associated with the plastic behaviour of the coating, are reported in Fig. 8. The hardness also increases with silica content, whatever the silica source. As observed for Young's modulus, coatings containing silica originating from TEOS exhibit the highest hardness.

The data scattering increases with silica content.

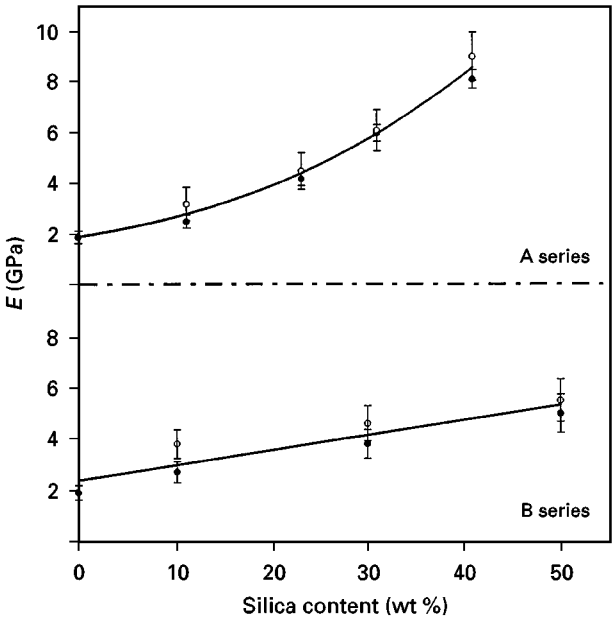

Figure 7 Young's modulus evolution as a function of the silica content determined by (○) flexion or (●) indentation experiment.

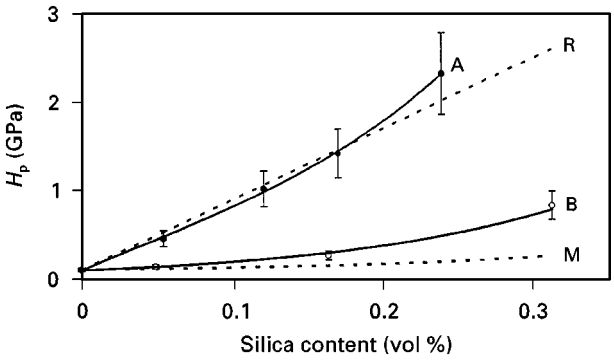

Figure 8 Hardness evolution as a function of the silica quantity. Comparison with Rice (R) and Myata (M) models.

4. Discussion

Properties such as erosion rate, impact resistance or scratching abrasion, are a combination of other well-defined properties, such as Young's modulus, hardness, toughness and stiffness. New coatings are now made of nanocomposites in which the different constituent compounds may be varied to achieve the required property. Thus it seems advantageous to establish the relations between the well-defined properties and the coating composition.

As expected, the addition of a mineral compound (silica) to an organosilicate polymer (GPTMS) induces an increase of Young's modulus. The elastic modulus of silica glass is about 70 GPa while that of polymerized GPTMS is 1.9 GPa. Most of the elastic models are expressed using the volume per cent of species. The density of silica is 2.2 g cm^{-3} and that of polymerized GPTMS is about 1.1 g cm^{-3}.

Elastic properties of a two-phase material may be estimated using various models. The simplest ones are those of Voigt (V) [18] and Reuss (R) [19]. They describe the mechanical behaviour of hypothetical two-phase composites. Voigt's model assumes that the deformation of the stressed composite is supported by both the matrix and the dispersed phase. Young's modulus of the composite is then

$$E = \tau_m E_m + \tau_r E_r \tag{8}$$

where τ is the volume fraction and the subscripts m and r correspond to the matrix and the inclusion.

Conversely, Reuss model assumes that matrix and reinforcement suffer the same stress. The elastic modulus is given by the relationship

$$E = \left(\frac{\tau_m}{E_m} + \frac{\tau_r}{E_r} \right)^{-1} \tag{9}$$

The two models mentioned above correspond to well-oriented phases as far as the direction of the stress is concerned. The Hashin and Shtrikman (HS) model ignores the geometrical details of the two-phase material [20]. This model is probably more suitable to describe elastic properties, and gives the boundaries within which the bulk and shear moduli of a composite should be found. These boundaries can be evaluated for composites for which K_r and G_r reinforcement are, respectively, higher than those of the matrice, K_m and G_m.

These two equations may be associated, to calculate Young's modulus according to the relation

$$E = \frac{9KG}{3K + G} \tag{10}$$

Young's modules of the coatings is located between the limits calculated from the HS model (Fig. 9). The curves obtained for the simplest models (R and V) are depicted in the same figure. Coatings (B) have a modulus which increases with the silica content according to the lowest HS limit. This feature agrees well with results obtained for a composite having a polymer matrix in which glass particles are dispersed [21–23]. This relatively low modulus may indicate that the colloidal particles are not strongly bonded to the GPTMS matrix. Colloidal particles must bear a limited number of silanol groups which must be able to react with those formed from hydrolysis reaction of GPTMS. It is likely that the stress is mainly supported by the matrix and reinforcement plays a little role.

Coatings prepared according to series A have an elastic modulus which increases very rapidly with silica content. Their values are found on the side of the highest HS limit. The difference between the two series appears clearly for silica contents higher than 15%. In series A, TEOS may form a mineral three-dimensional network which can be connected to the GPTMS molecule via the Si–OH functional group appearing from the hydrolysis reaction of Si–OMe. The connections between the mineral network and the organic network are more numerous. The entanglement between these two kinds of network is more efficient and induces a higher elastic modulus.

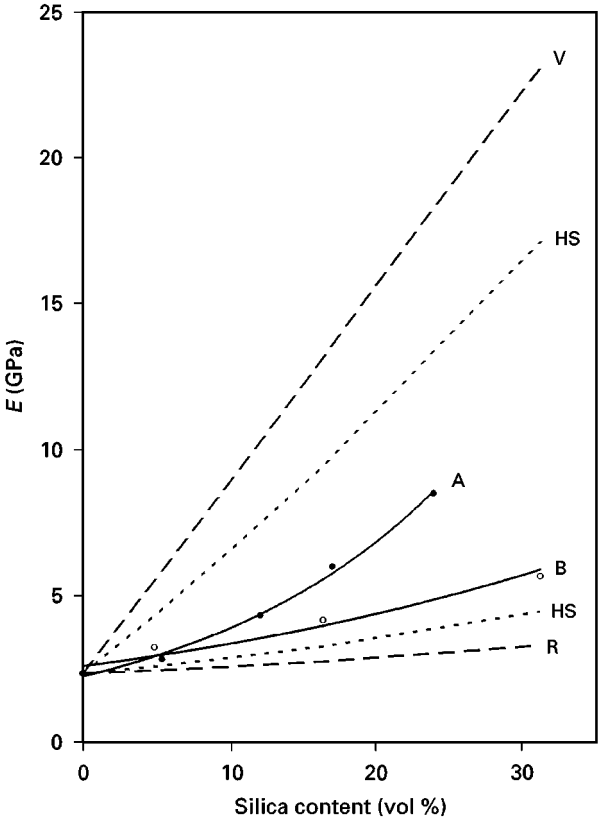

Figure 9 Young's modulus evolution as a function of the silica quantity. Comparison with Voigt (V), Reuss (R), and Hashin and Shtrikman (HS) models.

The highly different behaviour of these two kinds of coating is closely related to the way silica is positioned within the GPTMS network. It is worth noting that theoretical models do not perfectly describe Young's modulus variation, even if some analogies with HS boundaries are found. On the other hand, no evolution of Young's modulus of the series B is observed for a silica content higher than 20%. This value approximately corresponds to the three-dimensional percolation threshold for a disordered system [24].

Above the percolation threshold, Young's modulus is expected to change linearly with the volume per cent [25], because the elasticity must be mainly controlled by the hard phase and not by the soft matrix. This behaviour was not observed for our experiments which show a linear dependence of Young's modulus on the volume per cent up to 30%.

The hardness of the coatings obviously increases with the silica content of the layer (Fig. 8).

There are several models accounting for hardness variation with the volume fraction in nanocomposites. They require that the area investigated by the indentor is much broader than that of individual elements which constitute the composite coating. The simplest one is that of Rice (R) who assumes that the hardness linearly depends on the volume fraction [26]. Thus

$$\begin{aligned} H &= r_m H_m + \tau_r H_r \\ &= H_m + \tau_r (H_r - H_m) \end{aligned} \tag{11}$$

In the literature [27, 28] and commercial data [29], the value, H_r, of dense silica glass ranges from 6.5–9.5

GPa. Therefore, a mean value of 8 GPa was chosen, while the measured value of the GPTMS matrix is 100 MPa. The curve labelled R is drawn in Fig. 8.

Another model has been previously reported [30] to account for the hardness of a composite constituted by a glass matrix and spherical particles of ceramics. This model assumes that both the matrix and the dispersed material are homogeneous and isotropic. The matrix must behave as an elastic medium. This model must apply, as long as the volume fraction of the dispersed phase does not surpass the percolation threshold.

We must underline that the composite hardness value depends on the matrix elastic yield, σ_{ym}. The hardness is given by the relations

$$H = H_m \left\{ \left(1 + \frac{Q-1}{1-v_r Q} v_r \right) \times \left[1 + K \ln \frac{1 - v_r Q}{(1 - \alpha v_r)(1 - v_r)} \right] \right\} \quad (12a)$$

with

$$K = B \frac{\sigma_{ym}}{H_m} \quad (12b)$$

$$Q = \frac{15(1-\tau_m)G_r}{(7-5\tau_m)G_m + (8-10\tau_m)G_r} \quad (12c)$$

$$\alpha = \left(1 - \frac{G_m}{G_r} \right) Q \quad (12d)$$

B is a constant, equal to 0.6 [31]. The elastic yield stress, σ_{ym}, of the GPTMS matrix was estimated with the H_m/σ_{ym} ratio which is known to be equal to about 2 in polymers [30]. Thus, the estimated values of σ_{ym} is about 50 MPa. Poission's coefficient of GPTMS is assumed to be close to 0.4 [30] and that of silica 0.2 [27].

A comparison between the hardness of the two series of coatings shows that the models may be applied up to about 17% silica. Above this volume fraction, agreement no longer exists. The discrepancy between models and experimental data appears at a silica content close to the percolation threshold. Models are no longer valid because the infinite cluster made of the denser phase is now able to support the stress, and the matrix plays a minor role.

Coatings A follow Rice's model founded on the additive properties of the components. The coating is really a mixture of silica clusters entangled within a polymer matrix. The hardness of the coating agrees well with the M model, as long as it applies with respect to the initial hypothesis.

Moreover, we must underline that these models were applied to glasses and ceramics composites. Our system, whose properties are much closer to polymers, presents delayed elasticity and large deformation under the indentor tip at room temperature. Thus, to be more reliable, new models must be found to fit such a mechanical behaviour.

5. Conclusion

Young's modulus and the hardness of nanocomposite coatings have been measured using home-made equipment which permits the variation of these properties with the silica content, to be followed. Two different kinds of nanocomposite coatings were prepared and measured. These coatings can be regarded as models with respect to their respective manner to prepare a nanocomposite. One is prepared from a real mixture in which silica consists of dense particles, the second one is a composite made of entangled clusters of several hundred nanometres. Depending on the composite microstructure, different models accounting for the investigated properties may be used. The discrepancy between models and experimental values is low for silica contents lower than 20%, which is the percolation threshold of disordered material in three dimensions. Above this value, models must be used with caution. Consequently, it is possible to predict Young's modulus and hardness of nanocomposite coatings with respect to the details of the liquid mixture preparation. These values may be further used to obtain other properties such as erosion rate or scratching resistance.

Acknowledgements

The authors gratefully acknowledge the continuing aid of ESSILOR Research Department.

Appendix

Let us consider a coated sample in a three-point bending experiment (Fig. A1). Assuming a perfect adhesion between the substrate and the coating, we can write the longitudinal strength, σ_x, as a function of y [16]

$$\sigma_x = \frac{E_y(y - y_0)}{r} \quad (A1)$$

where E_y is Young's modulus of the material at the position, y, y_0 the neutral axis position, and r the radius of curvature.

On a surface element dA at a distance $y - y_0$ from the neutral axis, there is a force equilibrium along the x axis

$$\sum F = 0 \quad (A2)$$

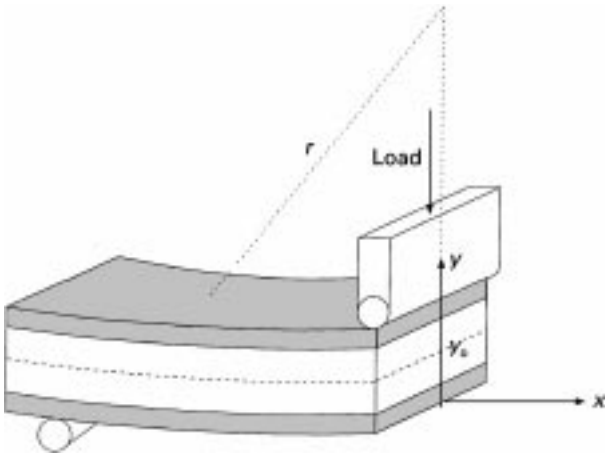

Figure A1 Beam deformation during the flexion experiment.

$$\Leftrightarrow \iint_A \sigma_x \cdot dA = 0 \tag{A3}$$

$$\Leftrightarrow \iint_A \frac{E_y(y - y_o)}{r} dA = 0 \tag{A4}$$

with $dA = b$ by

$$\Leftrightarrow \frac{1}{r}\left[\int_0^h E_c(y - y_0)\,dy + \int_{h_c}^{h_c+h_s} E_s(y - y_0)\,dy + \int_{h_c+h_s}^{2h_c+h_s} E_c(y - y_0)\,dy \right] = 0 \tag{A5}$$

$$\Leftrightarrow y_0 = \frac{2h_c + h_s}{2} \tag{A6}$$

Moreover, on the same surface element dA, there is an equilibrium of force moments along the x axis

$$\sum M = 0 \tag{A7}$$

$$\Leftrightarrow M_f - \iint_A \sigma \cdot (y - y_0)\,dA = 0 \tag{A8}$$

where M_f is the bending moment

$$\Leftrightarrow M_f = \iint_A \frac{E_y(y - y_0)^2}{r} dA = \frac{EI_z}{r} \tag{A9}$$

E is the apparent modulus of the sandwich with the moment of inertia

$$I_z = \frac{b(2h_c + h_s)^2}{12} \tag{A10}$$

Then

$$EI_z = E_c b \int_0^{h_c} (y - y_0)^2\,dy + E_s b \int_{h_c}^{h_z+h_s} (y - y_0)^2\,dy + E_c b \int_{h_c+h_s}^{2h_c+h_s} (y - y_0)^2\,dy \tag{A11}$$

and

$$E = E_S \frac{h_S^3}{(h_S + 2h_C)^3} + 2E_C \frac{h_C^3}{(h_S + 2h_C)^2} + 6E_C \frac{h_C(h_S + h_C)^2}{(h_S + 2h_C)^3} \tag{A12}$$

References

1. B. J. BRISCOE and D. TABOR, *Br Polym. J.* **10** (1978) 54.
2. H. DISLICH and E. HUSSMAN, *Thin Solid Films* **77** (1981) 129.
3. C. J. BRINKER and G. W. SCHERER, "Sol-Gel Science" (Academic Press, New York, NY, 1990).
4. D. C. BRADLEY, R. C. MEHROTRA and D. P. GAUR, "Metal alkoxides" (Academic Press, New York, NY, 1978).
5. H. SCHMIDT, *J. Non-Cryst. Solids* **73** (1985) 681.
6. P. ETIENNE, J. DENAPE, J. Y. PARIS, J. PHALIPPOU and R. SEMPERE, *J. Sol-Gel Sci. Technol.* **6** (1996) 287.
7. M. BUIJS, *J. Am. Ceram. Soc.* **77** (1994) 1676.
8. T. HANADA, Y. BESSYO and N. SOGA, *J. Non-Cryst. Solids* **113** (1989) 213.
9. A. HADDALENA and A. RACCANELLI, *ibid.* **151** (1992) 115.
10. D. SCHWEIDER, T. SCHWARZ and B. SCHULTRICH, *Thin Solid Films* **219** (1992) 92.
11. P. ETIENNE, R. SEMPERE and J. PHALIPPOU, *J. Sol-Gel Sci. Technol.* **2** (1994) 171.
12. J. L. LOUBET, J. M. GEORGES, O. MARCHESINI and G. MEILLE, *J. Tribol.* **106** (1984) 43.
13. D. FABES and W. C. OLIVER, *J. Non-cryst. Solids* **121** (1990) 348.
14. E. S. BERKOVICH, *Ind. Diamond Rev.* **11** (1951) 129.
15. M. F. DOERNER and W. D. NIX, *J. Mater. Res.* **1** (1986) 601.
16. S. TIMOSHENKO, "Strength of materials", Parts 1 and 2 (Van Nostrand, New York, NY, 1935).
17. B. SCHERRER, "Biostatistique" (Gaëtan Morin, Quebec, 1984).
18. W. VOIGT, in "Lehrbuch der Kristallophysik" (ed. Teubner, Berlin, 1910).
19. W. REUSS, *Z. Angew. Math. Mech.* **9** (1929) 49.
20. Z. HASHIN and S. SHTRIKMAN, *J. Mech. Phys.* **11** (1963) 127.
21. O. ISHAI and L. J. COHEN, *Int. J. Mech. Sci.* **9** (1967) 539.
22. J. C. SMITH, *Polym. Eng. Sci.* **16** (1976) 394.
23. T. G. RICHARD, *J. Mater. Sci* **9** (1975) 108.
24. D. STAUFFER, *Phys. Rev.* **54** (1979) 1.
25. M. I. GAI, L. I. MANEVICH and V. G. OSHMIAN, *Sov. Phys. Dokl.* **29** (1984) 505.
26. R. W. RICE, *J. Mater. Sci.* **14** (1979) 2768.
27. "SUPRASIL, Optical transparent fused silica", (Heraeus S.A, Z.A. Countaboenf-BP18 F-91941 Les ULIS Cedex, France), Edition 1994.
28. N. MIYATA and H. JINNO, *J. Mater. Sci.* **17** (1982) 547.
29. D. M. MARCH, *Proc. R. Soc. Lond.* **A279** (1964) 410.
30. D. TABOR, *Rev. Phys. Tech.* **1** (1970) 145.

Received 27 November 1996
and accepted 22 April 1998